Fracture assessment of magnetostrictive materials

M. Peron, S.M.J. Razavi, F. Berto, J. Torgersen
Department of Mechanical and Industrial Engineering, Norwegian University of Science and Technology (NTNU), Richard Birkelands vei 2b, 7491, Trondheim, Norway.
mirco.peron@ntnu.no, javad.razavi@ntnu.no, filippo.berto@ntnu.no, jan.torgersen@ntnu.no

M. Colussi
Department of Engineering and Management, University of Padova, Stradella S. Nicola 3, 36100, Vicenza (Italy)

ABSTRACT. Giant magnetostrictive materials are gaining interest in the field of smart material, especially the commercially known Terfenol-D, that is an alloy made out of iron, terbium and dysprosium ($Tb_{0.3}Dy_{0.7}Fe_{1.9}$). Since these smart materials are subjected to both mechanical loads and magnetic field during their industrial applications, an extensive characterization on the influence of a magnetic field and of defects on their fracture behavior is needed. Very few works can be found in literature about this topic and, thus, the purpose of this work is to partially fill this lack by means of three-point bending tests on single-edge pre-cracked Terfenol-D specimens. Failure loads have been measured at different loading rates and under magnetic fields of various intensities. Since giant magnetostrictive materials are very brittle, the strain energy density (SED) approach has been exploited by means of couple-field finite element analyses. SED has revealed itself as a robust parameters in the assessment of the magnetic field and loading rate effects on fracture resistance, allowing also to propose a relationship between the radius of the control volume and the loading-rate.

KEYWORDS. Strain energy density; Fracture toughness; Loading rates; Magnetic field; Giant magnetostrictive materials; Terfenol-D.

OPEN ACCESS

Citation: Peron, M., Razavi, S.M.J., Berto, F., Torgersen, J., Colussi, M., Fracture assessment of magnetostrictive materials, Frattura ed Integrità Strutturale, 42 (2017) 223-230.

Received: 15.07.2017
Accepted: 17.08.2017
Published: 01.10.2017

INTRODUCTION

Automotive industry, avionics and robotics are constantly looking for innovations, especially in the field of sensors, actuators and energy harvesting devices where smart material, such as magnetostrictive materials, are widely exploited [1]. This kind of material can convert magnetic energy into kinetic energy, i.e. it exhibits deformation once an external magnetic field is applied, or the reverse, i.e. an applied force determines a magnetization change. Such industrial applications require remarkable elongation and high energy density capacity at room temperature, features widely

present in the $Tb_{0.3}Dy_{0.7}Fe_{1.9}$ alloy, commercially known as Terfenol-D. Thus, among all the giant magnetostrictive materials, the ($Tb_{0.3}Dy_{0.7}Fe_{1.9}$) alloy has broadly gained interest in the last years.
However, despite of the great attention that this alloy has gained in the industrial applications and though it is susceptible to in-service fracture due to its brittleness [2], very few works are available concerning the assessment of the influence of manufacturing induced defect and cracks on magnetostricitve material performances, notwithstanding the widely reported harmful effects of notches [3–5]. Moreover, the fracture behavior of these materials are highly affected by the presence of magnetic fields, since the fracture resistance uder mode I is inversely related to the intensity of the field Narita et al. [6].
Regarding the determination of the fracture behavior of different materials, it is widely reported that brittle and high-cycle fatigue failures of components weakened by different notches geometries occur when the strain energy density (SED) averaged in a control volume surrounding a crack or notch tip reaches a critical value [7-15]. Colussi et al. [16] showed that this criterion could be extended also to giant magnetostrictive materials, under mode I loading condition, employing a control volume having radius 0.07 mm.
In this work, three point bending tests on Terfenol-D have been carried out, assessing the failure load at different loading rates both in presence and absence of an applied magnetic field. Then, coupled-field finite element analysis have been performed in order to evaluate the effect of the loading rate and of the magnetic field, allowing the development of a relationship between the critical radius R_c of the control volume and the loading rate.

ANALYSIS

Basic equations of the material

The basic equations for magnetostrictive materials are outlined as follows. Considering a Cartesian coordinate system, $O\text{-}x_1\,x_2\,x_3$, the equilibrium equations are given by:

$$\begin{aligned} &\sigma_{ji,j} = 0; \\ &\varepsilon_{ijk} H_{k,j} = 0; \\ &B_{i,i} = 0 \end{aligned} \tag{1}$$

where σ_{ji}, H_i and B_i are respectively the components of the stress tensor, the intensity vector of the magnetic field and the magnetic induction vector, whereas ε_{ijk} is the Levi-Civita symbol. A comma followed by an index denotes partial differentiation with respect to the spatial coordinate x_i and the Einstein's summation convention for repeated tensor indices is applied. The constitutive laws are given as:

$$\begin{aligned} \varepsilon_{ij} &= s^H_{ijkl}\sigma_{kl} + d_{kij}H_k \\ B_i &= d_{ikl}\sigma_{kl} + \mu^T_{ik}H_k \end{aligned} \tag{2}$$

where ε_{ij} are the components of the strain tensor and $s^H_{ijkl}, d_{ikl}, \mu^T_{ik}$ are respectively the magnetic field elastic compliance, the magnetoelastic constants and the magnetic permittivity. Valid symmetry conditions are:

$$\begin{aligned} &s^H_{ijkl} = s^H_{jikl} = s^H_{ijlk} = s^H_{klij} \\ &d_{kij} = d_{kji} \\ &\mu^T_{ij} = \mu^T_{ji} \end{aligned} \tag{3}$$

The relation between the strain tensor and the displacement vector u_i is:

$$\varepsilon_{ij} = \frac{1}{2}\left(u_{j,i} + u_{i,j}\right) \tag{4}$$

The magnetic field intensity, named φ the potential, is written as:

$$H_i = \varphi_{,i} \tag{5}$$

For Terfenol-D, the constitutive relations can be written as:

$$\begin{Bmatrix} \varepsilon_{11} \\ \varepsilon_{22} \\ \varepsilon_{33} \\ 2\varepsilon_{23} \\ 2\varepsilon_{31} \\ 2\varepsilon_{12} \end{Bmatrix} = \begin{bmatrix} s_{11}^H & s_{12}^H & s_{13}^H & 0 & 0 & 0 \\ s_{12}^H & s_{11}^H & s_{13}^H & 0 & 0 & 0 \\ s_{13}^H & s_{13}^H & s_{33}^H & 0 & 0 & 0 \\ 0 & 0 & 0 & s_{44}^H & 0 & 0 \\ 0 & 0 & 0 & 0 & s_{44}^H & 0 \\ 0 & 0 & 0 & 0 & 0 & s_{66}^H \end{bmatrix} \begin{Bmatrix} \sigma_{11} \\ \sigma_{22} \\ \sigma_{33} \\ \sigma_{23} \\ \sigma_{31} \\ \sigma_{12} \end{Bmatrix} + \begin{bmatrix} 0 & 0 & d_{31} \\ 0 & 0 & d_{31} \\ 0 & 0 & d_{33} \\ 0 & d_{15} & 0 \\ d_{15} & 0 & 0 \\ 0 & 0 & 0 \end{bmatrix} \begin{Bmatrix} H_1 \\ H_2 \\ H_3 \end{Bmatrix} \tag{6}$$

$$\begin{Bmatrix} B_1 \\ B_2 \\ B_3 \end{Bmatrix} = \begin{bmatrix} 0 & 0 & 0 & 0 & d_{15} & 0 \\ 0 & 0 & 0 & d_{15} & 0 & 0 \\ d_{31} & d_{31} & d_{33} & 0 & 0 & 0 \end{bmatrix} \begin{Bmatrix} \sigma_{11} \\ \sigma_{22} \\ \sigma_{33} \\ \sigma_{23} \\ \sigma_{31} \\ \sigma_{12} \end{Bmatrix} + \begin{bmatrix} \mu_{11}^T & 0 & 0 \\ 0 & \mu_{11}^T & 0 \\ 0 & 0 & \mu_{33}^T \end{bmatrix} \begin{Bmatrix} H_1 \\ H_2 \\ H_3 \end{Bmatrix} \tag{7}$$

where:

$$\left.\begin{aligned} &\sigma_{23} = \sigma_{32}\ ,\ \sigma_{31} = \sigma_{13}\ ,\ \sigma_{12} = \sigma_{21} \\ &\varepsilon_{23} = \varepsilon_{32}\ ,\ \varepsilon_{31} = \varepsilon_{13}\ ,\ \varepsilon_{12} = \varepsilon_{21} \end{aligned}\right\}$$

$$\left.\begin{aligned} &s_{11}^H = s_{1111}^H = s_{2222}^H\ ,\ s_{12}^H = s_{1122}^H\ ,\ s_{13}^H = s_{1133}^H = s_{2233}^H\ ,\ s_{33}^H = s_{3333}^H \\ &s_{44}^H = 4s_{2323}^H = 4s_{3131}^H\ ,\ s_{66}^H = 4s_{1212}^H = 2\left(s_{11}^H - s_{12}^H\right) \end{aligned}\right\}$$

$$d_{15} = 2d_{131} = 2d_{223}\ ,\ d_{31} = d_{311} = d_{332}\ ,\ d_{33} = d_{333}$$

Averaged Strain Energy Density (SED) approach

According to Lazzarin and Zambardi [10], the brittle failure of a component occurs when the total strain energy, $\bar{W}$, averaged in a specific control volume located at a notch or crack tip, reaches the critical value W_c. In agreement with Beltrami [17], named σ_t the ultimate tensile strength under elastic stress field conditions and E the Young's modulus of the material, the critical value of the total strain energy can be determined by the following:

$$W_c = \frac{\sigma_t^2}{2E} \tag{8}$$

The control volume takes different shapes based on the kind of notch. If the notch is represented by a crack, its opening angle is equal to zero and the control volume is a circumference of radius R_c, centered on the crack tip. Being this the case, the radius R_c can be evaluated once known the fracture toughness, K_{IC}, the tensile stress and the Poisson's ratio, ν, of the material, by means of the following expression proposed by Yosibash et al. [18]:

$$R_c = \frac{(1+\nu)(5-8\nu)}{4\pi}\left(\frac{K_{IC}}{\sigma_t}\right)^2 \tag{9}$$

The SED averaged in the control volume can be computed directly by means of a finite element analysis.

Finite element model

In order to compute the averaged strain energy density, $\bar{W}$, analyses were performed by means of ANSYS R14.5 finite element code, both in plane strain and plane stress conditions depending on the specimens' width. For the purpose, solid models were used to determine which was the most appropriate condition.

As shown by Tiersten [19], the basic equations for magnetostrictive materials are mathematically equivalent to those of the piezoelectric materials, so four nodes PLANE13 and eight node SOLID5 coupled-field solid elements from ANSYS'

library were used, respectively for plane and solid models, and the magnetic field has been introduced by a voltage difference. The coordinate axes $x = x_1$ and $z = x_3$ are chosen such that the $y = x_2$ axis coincides with the thickness direction and such that the easy axis of magnetization is the z-direction. Because of symmetry, only the half of the model was used in the FEA.

Before carrying out simulations, a mesh sensitivity study was undertaken to determine the adequate finite element (FE) number to be used. SED value have been first determined from a very refined mesh and then from some coarser meshes. The refined mesh had the same FE number adopted in a previous work by the authors, in which finite element models with 6400 elements were used to evaluate the energy release rate by means of J-integral on the same geometry. Among different coarse mesh patterns, it has been found suitable for compute SED without accuracy lost a mesh with 274 elements, of which at 10 elements placed inside the control volume. The results are summarized in Tab. 1, where the SED value from the proposed coarse mesh is compared with that from the very refined one. The mesh insensitivity is a consequence of the finite element method, in which the elastic strain energy is computed from the nodal displacements, without involving stresses and strains, as shown by Lazzarin et al. [10].

The relationship between magnetostriction and magnetic field intensity is essentially non-linear. Nonlinearity arises from the movement of the magnetic domain walls, as shown by Wan et al. [20]. To take into account this non-linear behavior, the constants d_{15}, d_{31} and d_{33} for Terfenol-D, in presence of $B_z = B_0$, are given by:

$$\begin{aligned} d_{15} &= d_{15}^{m} \\ d_{31} &= d_{31}^{m} + m_{31} H_z \\ d_{33} &= d_{33}^{m} + m_{33} H_z \end{aligned} \tag{10}$$

where d_{15}^{m}, d_{31}^{m} and d_{33}^{m} are the piezomagnetic constants, whereas m_{31} and m_{33} are the second order magnetoelastic constants. Jia et al. [21] proved that if the specimen's dimension in the direction in which the magnetic field is applied is at least two times greater than the other two dimensions, then the longitudinal magnetostriction is prevailing and it can be assumed that only d_{33} is a function of the magnetic field H_z and that m_{31} is equal to zero.

Number FE (control volume)	Control volume	Control volume	Number FE model)	$\bar{W}$ [MJ.m^{-3}]	$\Delta\bar{W}$ [%]
128	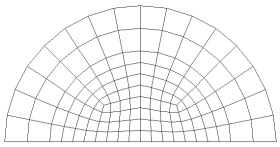	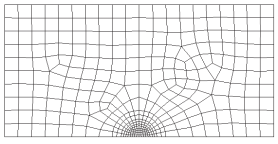	6400	0.01461	-
10	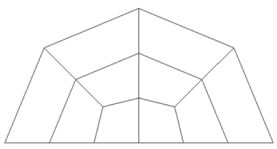	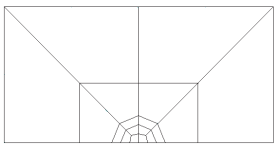	274	0.01457	-0.3

Table 1: Mean values of *SED* for different mesh refinement.

Material	Elastic compliance [10^{-12} m^2.N^{-1}]					Piezo-magnetic constants [10^{-9} mA^{-1}]			Magnetic permeability [10^{-6} Hm^{-1}]		Density [kg.m^{-3}]
	S_{11}^{H}	S_{33}^{H}	S_{44}^{H}	S_{12}^{H}	S_{13}^{H}	d_{31}^{m}	d_{33}^{m}	d_{15}^{m}	μ_{11}^{T}	μ_{33}^{T}	ϱ
Terfenol-D	17.9	17.9	26.3	-5.88	-5.88	-5.3	11	28	6.29	6.29	9250

Table 2: Terfenol-D material properties.

EXPERIMENTAL PROCEDURE

Among giant magnetostrictive materials, the commercially named Terfenol-D alloy, supplied by Etrema Products, Inc. (USA) was used in all tests and analyses. The material properties are listed in Tab. 2.
Test were performed with the aim to measure the fracture load, P_c, of single edge precracked specimens, subjected to three point bending, in presence and in absence of the magnetic field and at various loading-rates. Specimens were 5 mm thick, 3 mm wide and 15 mm long. Before testing, all specimens were weakened on one side by a 0.5 mm deep crack, which was introduced using a tungsten cutter. Tested specimen is showed in Fig. 1.

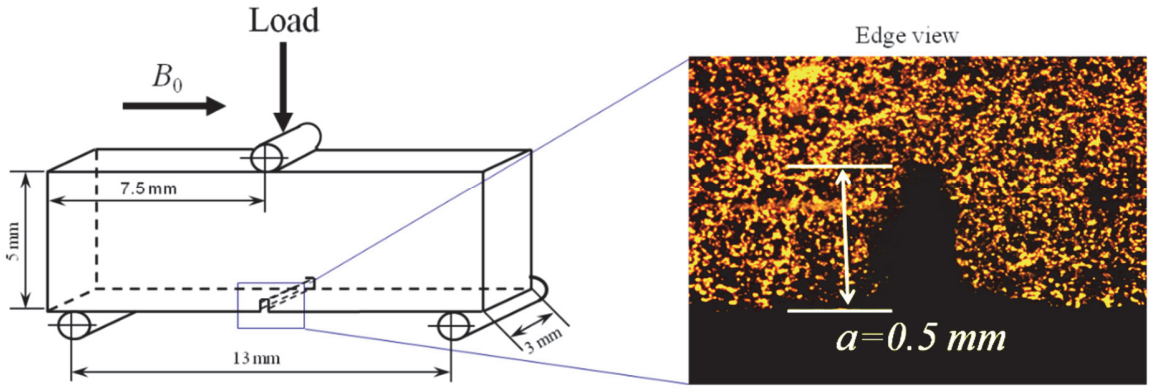

Figure 1: Specimen's geometry and edge micrograph of the introduced crack.

The load P has been impressed at the midpoint of the specimens, which were simply supported with span of 13 mm, by means of a 250 N load cell (resolution: 0.01 N). The load was applied for different loading-rates: 0.05, 0.5 and 3.0 Ns^{-1}. A uniform magnetic field, with magnetic induction B_0, has been applied in the longitudinal direction through an electromagnet. As devices in which Terfenol-D is employed commonly work in magnetic induction range which varies from 0.02 T to 0.05 T, the representative value of 0.03 T has been adopted in all tests. It is due to point out that, as alloying elements in Terfenol-D are Terbio and Disprosio, which are very expensive rare earths, the number of tested specimens was limited: from two to three at each condition.
By means of experimental procedure it has also been possible to assess the second order magnetoelastic constant, m_{33}. Let consider a Cartesian coordinate system, O-x y z, which origin is located at the top center of an uncracked specimen. Varying the intensity of the magnetic field applied in the z-direction (longitudinal direction), the trend of magnetostriction has been measured through a strain gauge located at $x = y = z = 0$ mm. By comparison between the measured strain ε_{zz} and the numerically obtained one, it has been found that the proper value for the second order magnetoelastic constant is 4.82×10^{-12} m^2A^{-2}. This value has been used in the analyses to compute the SED.

RESULTS AND DISCUSSION

Fracture load, P_c, in presence and absence of the magnetic field have been experimentally measured at each loading-rate. Data, in terms of fracture load, are summarized in Tab. 3. Bold numbers represent the average value at each condition, whereas numbers in brackets represent the relative standard deviations.
Average fracture loads are presented in Fig. 2. The error bars indicate the maximum and minimum values of P_c. The average fracture load at 0.05 Ns^{-1}, 0.50 Ns^{-1} and 3.0 Ns^{-1} are decreased respectively about 7%, 9% and 14% in the presence of the magnetic field. It has also been found that Terfenol-D shows a decrease in fracture load as the loading-rate decreases. Similar behavior has been observed for other materials such as TiAl alloys, by Cao et al. ([22]) and piezoelectric ceramics, by Shindo et al. ([23-24]) and Narita et al. ([25]).
To take into account the effect of the loading-rate on Terfenol-D fracture load, here it is assumed that the critical radius R_c, which depends on the material and on the notch opening angle, varies also with the speed at which the load is applied. By plotting the averaged SED related to the mean values of critical loads in Tab. 3, in presence and in absence of the magnetic field, as a function of control volume radius, it is possible to determine different intersections for each loading-rate. The intersections have been found at 0.05, 0.056 and 0.1 mm respectively for the loading-rates 0.05, 0.5 and 3.0 Ns^{-1}.

This means that, at the critical load, the material is characterized by a value of strain energy density, averaged in a control volume having size variable with the loading-rate, which is independent of the ratio between the applied load and magnetic field. A good fit of R_c versus loading-rate to a linear model has been found, then, adopting a simple linear regression model, the following relationship is proposed:

$$R_c = 0.0195\frac{dP}{dt} + 0.05 \tag{11}$$

dP/dt	P_c [N] B = 0 T	B = 0.03 T
0.05 Ns^{-1}	58.3	59.2
	65.8	61.9
	74.7	64.6
	66.3 (5.81)	**61.9** (1.91)
0.5 Ns^{-1}	66.6	60.7
	68.5	61.6
	67.5 (0.78)	**61.1** (0.37)
3.0 Ns^{-1}	71.0	74.2
	79.2	59.3
	-	60.0
	75.1 (3.35)	**64.5** (5.95)

Table 3: Measured fracture loads as a function of the loading-rate and the magnetic field

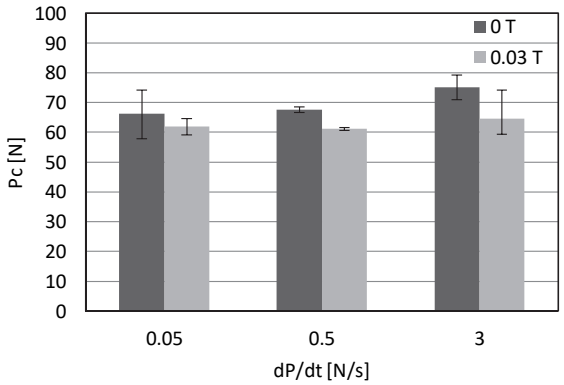

Figure 2: Mean fracture loads as a function of the loading-rate and the magnetic field

The approximated critical radius of 0.07 mm, obtained from (9) and suggested by Colussi et al. [16] without taking into account the loading-rate, falls amid of the range of variation here proposed.

Fig. 3 shows a summary of the experimental data in terms of the square root of the ratio between the averaged strain energy density, $\overline{W}$, and the critical value of strain energy, W_c. This parameter has been chosen because of its proportionality to the fracture load. The averaged strain energy density, $\overline{W}$, has been computed in control volumes having radius given by (11), whereas a critical strain energy equal to 0.02 MJ.m^{-3} is assumed. This critical value is obtained from Eq. (8), assuming Young's modulus equal to 30 GPa, Poisson's ratio equal to 0.25 and tensile strength equal to 34 MPa, which are the medium characteristics provided by the material supplier. Here, Young's modulus is assumed independent from the applied magnetic field. This assumption is reasonable in the range of variation of the applied magnetic field. In Fig. 3 experimental data from Narita et al. [25] have also been summarized. Data referred to fracture loads measured under three point bending, with and without magnetic a 0.03 T magnetic field, at the following loading-rate: 0.2 Ns^{-1} and 3.0 Ns^{-1}. Specimens were 3 mm thick, 5 mm wide and 15 mm long. Crack depth was 0.5 mm. Due to the different geometry (ratio between width and thickness equal to 5/3 instead of 3/5) plane strain condition instead of plane stress condition resulted more appropriate for their modeling. It has been found that about all experimental data fit in a narrow scatter band, which limits are drown here with an engineering judgment from 0.80 to 1.20 (4 data over 35

being outside of this range). The few data which exceed the band fall however in the safety region of the plot. The averaged SED criterion appears suitable for fracture strength assessment of cracked specimens made out of Terfenol-D alloy, under mode I condition, in presence or absence of the magnetic field and with variable loading-rate. In the authors' opinion the result is satisfactory and the SED criterion permits the reliable assessment of Terfenol-D brittle failure by means of coarse mesh based finite element models. The proposed relationship between the size of the control volume and the loading-rate also permit to take into account the loading-rate by means of static analyses. Some future developments will involve also high temperature applications [26].

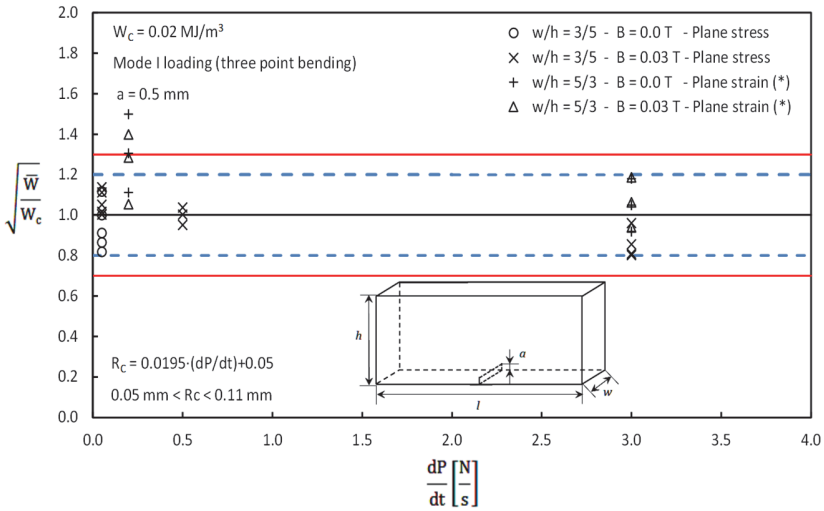

Figure 3: Mean fracture loads as a function of the loading-rate and the magnetic field B.

CONCLUSIONS

A combined experimental and numerical study was conducted to understand the defect sensitivity of giant magnetostrictive materials. Under mode I loading condition, it has been found that Terfenol-D shows a decrease in fracture load in presence of a magnetic field. This behavior in justified by the increase of the strain energy with increasing magnetic fields. Terfenol-D also shows a decrease in fracture loads as the loading-rate decreases. Results indicate that SED criterion in able to capture this behavior if a linear relationship between the size of the control volume and the loading-rate is assumed. A good match between experimental results and numerical predictions has been found and a substantial mesh insensitivity of SED approach has been proved.

REFERENCES

[1] Zhao, X., Lord, D.G., Application of the Villari effect to electric power harvesting, J. Appl. Phys., 99 (2006) 08M703
[2] Peterson, D.T., Verhoeven, J.D., McMasters, O.D., Spitzig, W.A., Strength of Terfenol-D. J. Appl. Phys., 65 (1989) 3712.
[3] Lazzarin, P., Comportamento a fatica dei giunti saldati in funzione della densità di energia di deformazione locale: influenza dei campi di tensione singolari e non singolari, Frattura ed Integrità Strutturale, 9 (2009) 13-26.
[4] Maragoni, L., Carraro, P. A., Peron, M. and Quaresimin, M., Fatigue behaviour of glass/epoxy laminates in the presence of voids, Int. J. Fatigue, 95 (2017) 18–28.
[5] Brotzu, A., Felli, F. and Pilone, D., Effects of the manufacturing process on fracture behaviour of cast TiAl intermetallic alloys, Fract. Struct. Integr. 27 (2013), 66-73.
[6] Narita, F., Morikawa, Y., Shindo, Y., Sato, M., Dynamic fatigue behavior of cracked piezoelectric ceramics in three-point bending under AC electric fields, J. Eur. Cera. Soc., 32 (2012) 3759–3766.
[7] Ayatollahi, M.R., Razavi, S.M.J., Rashidi Moghaddam, M., Berto, F., Mode I fracture analysis of Polymethylmetacrylate using modified energy—based models. Phys. Mesomec., 18 (2015) 53-62.

[8] Ayatollahi, M.R., Rashidi Moghaddam, M., Razavi, S.M.J., Berto, F., Geometry effects on fracture trajectory of PMMA samples under pure mode-I loading. Eng. Fract. Mech., 163 (2016) 449–461.
[9] Rashidi Moghaddam, M., Ayatollahi, M.R., Razavi, S.M.J., Berto, F., Mode II Brittle Fracture Assessment Using an Energy Based Criterion, Phys. Mesomec. (in press).
[10] Lazzarin, P. and Zambardi, R., A finite-volume-energy based approach to predict the static and fatigue behavior of components with sharp V-shaped notches, Int. J. Fract., 112 (2001) 275–298.
[11] Berto, F., Lazzarin, P. and Ayatollahi, M. R., Brittle fracture of sharp and blunt V-notches in isostatic graphite under torsion loading, Carbon N. Y., 50 (2012) 1942–1952.
[12] Radaj, D., Berto, F., and Lazzarin, P., Local fatigue strength parameters for welded joints based on strain energy density with inclusion of small-size notches, Eng. Fract. Mech., 76 (2009) 1109–1130.
[13] Berto, F., Croccolo, D. and Cuppini, R., Fatigue strength of a fork-pin equivalent coupling in terms of the local strain energy density, Mater. Des., 29 (2008) 1780–1792.
[14] Berto, F. and Barati, E., Fracture assessment of U-notches under three point bending by means of local energy density, Mater. Des., 32 (2011) 822–830.
[15] Berto, F. and Ayatollahi, M. R., Fracture assessment of Brazilian disc specimens weakened by blunt V-notches under mixed mode loading by means of local energy, Mater. Des., 32 (2011) 2858–2869.
[16] Colussi, M., Berto, F., Mori, K., Narita, F., Effect of the loading rate on the Brittle Fracture of Terfenol-D Specimens in Magnetic Field: Strain Energy Density Approach, Strength Mater, (in press).
[17] Beltrami, E., Sulle condizioni di resistenza dei corpi elastici, Rendiconti del Regio Istituto Lombardo XVIII, (1885) 704-714.
[18] Yosibash Z., Bussiba A. R., G.I., Failure criteria for brittle elastic materials. Int. J. Fracture, 125 (2004) 307–333.
[19] Tiersten, H.F., 1969. Linear piezoelectric plate vibrations: elements of the linear theory of piezoelectricity and the vibrations of piezoelectric plates. Springer, New York, (1969).
[20] Wan, Y., Fang, D., Hwang, K.C., Non-linear constitutive relations for magnetostrictive materials, Int. J. Nonlinear Mech., 38 (2003) 1053–1065.
[21] Jia, Z., Liu, W., Zhang, Y., Wang, F., G.D., A nonlinear magnetomechanical coupling model of giant magnetostrictive thin films at low magnetic fields, Sens. Actuators A, 128 (2006) 158-164.
[22] Cao, R., Lei, M.X., Chen, J.H., Zhang, J., Effects of loading rate on damage and fracture behavior of TiAl alloys. Mater. Sci. Eng., 465 (2007) 183–193.
[23] Shindo, Y., Mori, K., Narita, F., Electromagneto-mechanical fields of giant magnetostrictive / piezoelectric laminates. Acta Mech., 212 (2010) 253-261.
[24] Shindo, Y., Narita, F., Mori, K., Nakamura, T., Nonlinear bending response of giant magnetostrictive laminated actuators in magnetic fields, J. Mech. Mater. Struct., 4 (2009) 941–949.
[25] Narita, F., Morikawa, Y., Shindo, Y., Sato, M., Dynamic fatigue behavior of cracked piezoelectric ceramics in three-point bending under AC electric fields, J. Eur. Ceram. Soc., 32 (2012) 3759–3766.
[26] Gallo, P., Berto, F., Glinka, G Generalized approach to estimation of strains and stresses at blunt V-notches under non-localized creep, Fatigue Fract. Eng. Mater. Struct, 39 (2016) 292-306.